

## DYNAMICAL PERFORMANCE OF A BUS UNDER DIRECTIONAL MANEUVERNS

### Nilson Barbieri

Pontifícia Universidade Católica do Paraná – PUCPR – Rua Imaculada Conceição, 1155 – CEP: 80215-901 – Curitiba – PR  
nilson.barbieri@pucpr.br

### Renato Barbieri

Pontifícia Universidade Católica do Paraná – PUCPR – Rua Imaculada Conceição, 1155 – CEP: 80215-901 – Curitiba – PR  
nilson.barbieri@pucpr.br

### Claúdio Carreirão

Volvo do Brasil Veículos Ltda  
claudio.carreirao@volvo.com

**Abstract.** *The dynamical performance of a bus, under directional maneuver over a flat road is analyzed through a physical model with eight degrees of freedom. Non linearities coming from the brake and side forces developed on the tire contact patch are considered for the vehicle under directional maneuvers. The mathematical models are validated by comparisons between the experimental and simulated data. The experimental data are obtained through an accelerometer placed in the gravitational center at lateral direction and four displacement sensors placed in the vehicle suspensions. The parameters analyzed are lateral acceleration and roll angle.*

**Keywords** *directional maneuver, bus, lateral acceleration, roll angle*

### 1. Introduction

The behavior of the vehicle under the directional point of view was analyzed by Nardello, Benincá and Vargas (2000). The focus is directed to the experimental investigation, considering the effect of the use of the stabilizers bars and suspension dampers in different buses.

Allen et. al. (2002), created and validated experimentally, a computational model to preview the directional behavior of bus.

Brach (1991), developed a simple and flexible computational model capable to generate simulations of articulated and non articulated vehicles. This work uses the BNP model for the simulation of the tire lateral and brake forces. Allen, Rosenthal and Szostak (1987), developed a complex model considering the parameters that influence the generation of lateral and longitudinal force by the tire. A complex tire model was presented with details.

Shiller (1995) and Ramanata (1998) studied an intermediary area between control and directional dynamics. Both authors developed optimal vehicle path generator using directional control of the bicycle model for the vehicle with the Dugoff and Segel tire models. Smith and Starkey (1995) presented eight degrees of freedom vehicle model using the Dugoff's tire model.

In the area of directional control, Lee, Lee and Han (2001) and Lee and Han (2001), explored the effect of the control of the kinematics of the suspension, especially the roll center position.

Kwak and Park (2002) and Kwak and Park (2001), starting from a computational nonlinear model with 15 degrees of freedom, showed the benefits of a control system using traditional traction and variables of directional control.

Mangliardi and Mantriota (2001) analyzed possible conditions of instability that can be induced by the presence of oscillating cargo.

Diaz et. al (2004) introduced a new method based on a theoretical model and dynamics test establishing the rollover limit that a vehicle can reach without rolling. The equations of the model represent the vehicle dynamical behaviour when the bus is being driven on a curve. The results of the tests allow to characterise the behaviour, for real conditions on a turn, of many parameters involved in the model. The dynamic tests on the road and the mathematical model predict a reliable rollover limit of a bus. The knowledge of this value will increase the safety of these vehicles.

The main objective of this work is to analyze the lateral acceleration and the roll angle of a bus through eight degrees of freedom model. To analyze the dynamical performance of vehicle the forward speed was varied between 20 and 60 km/h. The experimental data was acquired through an accelerometer placed at the gravitational center in lateral direction and four displacement sensors placed in the suspensions in vertical direction. The simulated and experimental data are confronted to validate the mathematical model. Virtual design of new bus can be obtained through the computational simulations using the reliable mathematical model.

## 2. Vehicle model

All dynamic equations will be based on a inertial axis systems. Figure 8 shows the axis system for the sprung mass is denominated by " $x_s y_s z_s$ ". Besides this inertial axis system, it is necessary to have a earth fixed axis system denominated by " $X Y Z$ ". For the unsprung masses, similar inertial axis, denominated by " $x_u y_u z_u$ " was adopted and is shown on Fig 1.

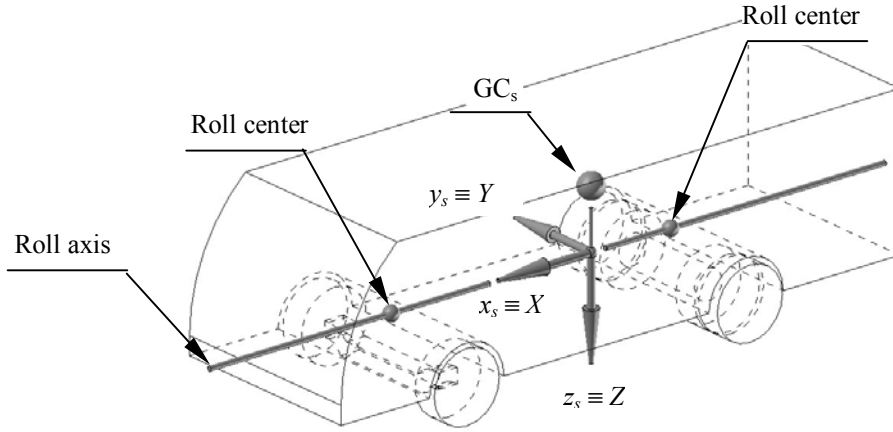


Figure 1. Sprung mass axis system

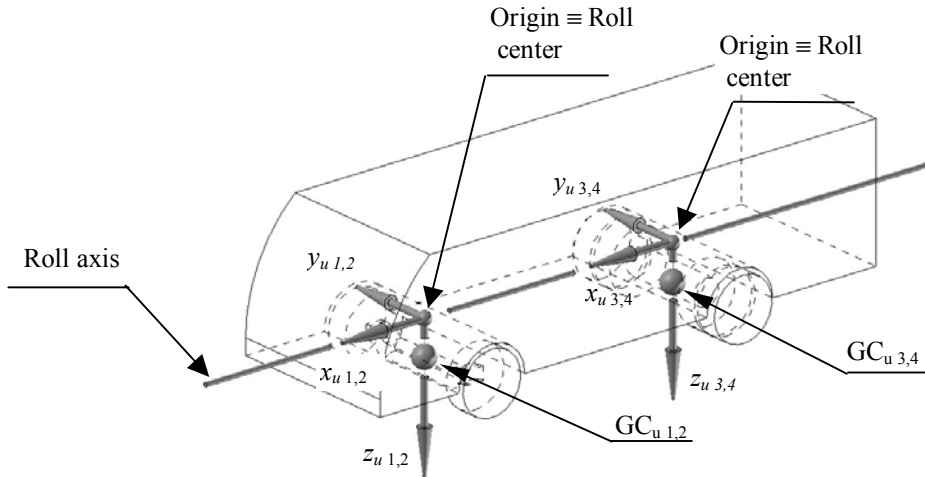


Figure 2. Unsprung axis system

The degrees of freedom of each axis system are:

- For the sprung mass axis system
  - Movement along " $x_s$ " and along " $y_s$ ";
  - Rotation around " $x_s$ " and around " $z_s$ ".
- For the unsprung axis system
  - Movement along " $x_u$ " and along " $y_u$ ";
  - Rotation around " $z_u$ ".

The sum of forces and moments on the inertial systems considering similar degrees of freedom and taking the assumption of symmetry and alignment with the principal inertia directions are (Ellis, 1994):

- For the sprung mass axis system

$$\Sigma Fx_s = m \cdot ax_s = m_s \cdot (\dot{u}_s - v_s \cdot r_s) + m_s \cdot \bar{z}_s \cdot p_s \cdot r_s \quad (1)$$

$$\Sigma Fy_s = m \cdot ay_s = m_s \cdot (\dot{v}_s + u_s \cdot r_s) - m_s \cdot \bar{z}_s \cdot \dot{p}_s \quad (2)$$

$$\Sigma Mx_s = Ix_s \cdot \dot{p}_s - m_s \cdot \bar{z}_s \cdot (\dot{v}_s + u_s \cdot r_s) \quad (3)$$

$$\Sigma Mz_s = Iz_s \cdot \dot{r}_s \quad (4)$$

where:  $m_s$  = sprung mass;  $Ix_s$  and  $Iz_s$  mass moment of inertia about longitudinal and vertical axes;  $u$ ,  $v$  and  $r$  = longitudinal, lateral e angular (about z axis) velocities;  $\dot{p}$  and  $\dot{r}$  are angular accelerations about x and z axes.

- For the unsprung mass axis systems

$$\Sigma Fx_u = m_u \cdot ax_u = m_u \cdot (\dot{u}_u - v_u \cdot r_u) \quad (5)$$

$$\Sigma Fy_u = m_u \cdot ay_u = m_u \cdot (\dot{v}_u + u_u \cdot r_u) \quad (6)$$

$$\Sigma Mz_u = Iz_u \cdot \dot{r}_u \quad (7)$$

It is possible to achieve some relations between the unsprung masses axis system and the sprung mass axis system variables, as shown on Eq. (8). These relations are used to found the system equations for the complete vehicle (including sprung and unsprung masses) using only the variables associated to the sprung mass axis system.

$$\begin{aligned} u_{u\ i,j} &= u_s \\ v_{u\ i,j} &= v_s + xp_{CGu\ i,j} \cdot r_s \\ r_{u\ i,j} &= r_s \end{aligned} \quad (8)$$

where  $xp_{CG}$  is the position of the gravity center.

After applying the equilibrium equations on the free body diagrams of the sprung and unsprung masses, and taking the assumption that the masses are connected by the suspension roll centers, a set of differential equations are achieved, and can be written in matrix form as:

$$[M] \cdot \{\ddot{\eta}\} + [C] \cdot \{\dot{\eta}\} + [K] \cdot \{\eta\} = \{F\} \quad (9)$$

where:

$$[M] = \begin{bmatrix} m_s + \sum_{i,j=1,2}^{m,n_u} m_{u\ i,j} & 0 & 0 & 0 \\ 0 & m_s + \sum_{i,j=1,2}^{m,n_u} m_{u\ i,j} & - \sum_{i,j=1,2}^{m,n_u} (m_{u\ i,j} \cdot xp_{CGu\ i,j}) & - m_s \cdot zp_{CGs} \\ 0 & 0 & Iz_s + \sum_{i,j=1,2}^{m,n_u} (Iz_{u\ i,j} + m_{u\ i,j} \cdot xp_{CGu\ i,j}^2) & 0 \\ 0 & - m_s \cdot zp_{CGs} & 0 & Ix_s \end{bmatrix} \quad (10)$$

$$[C] = \begin{bmatrix} 0 & -\left(m_s + \sum_{i,j=1,2}^{m,n_u} m_{u\ i,j}\right) \cdot r_s & -\left(\sum_{i,j=1,2}^{m,n_u} (m_{u\ i,j} \cdot xp_{CGu\ i,j})\right) \cdot r_s & m_s \cdot zp_{CGs} \cdot r_s \\ 0 & 0 & \left(m_s + \sum_{i,j=1,2}^{m,n_u} m_{u\ i,j}\right) \cdot u_s & 0 \\ 0 & 0 & 0 & 0 \\ 0 & 0 & -m_s \cdot zp_{CGs} \cdot u_s & \sum_{k=1}^{n_D} (CD_k \cdot yp_{Dk}^2) \end{bmatrix} \quad (11)$$

$$[K] = \begin{bmatrix} 0 & 0 & 0 & 0 \\ 0 & 0 & 0 & 0 \\ 0 & 0 & 0 & 0 \\ 0 & 0 & 0 & \sum_{i,j=1,2}^{m,n_u} (CSB_{i,j}) + \sum_{k=1}^{n_{AS}} (CK_k \cdot yp_{Kk}^2) + m_s \cdot g \cdot zp_{CGs} \end{bmatrix} \quad (12)$$

$$\{F\} = \left\{ \begin{array}{l} \sum_{t=1}^{n_T} FTx_t - EFF \\ \sum_{t=1}^{n_T} FTy_t + EFL \\ \sum_{k=1}^{n_T} (FTy_k \cdot xp_{T\ k}) - \sum_{k=1}^{n_T} (FTx_k \cdot yp_{T\ k}) + EFF \cdot yp_{EFF} + EFL \cdot xp_{EFL} \\ - EFL \cdot zp_{EFL} - \sum_{k=1}^{n_D} (BD_k \cdot yp_{Dk}) - \sum_{k=1}^{n_{AS}} (BB_k \cdot yp_{Kk}) \end{array} \right\} \quad (13)$$

$$\{\ddot{\eta}\} = \begin{Bmatrix} \dot{u}_s \\ \dot{v}_s \\ \dot{r}_s \\ \dot{p}_s \end{Bmatrix}; \quad \{\dot{\eta}\} = \begin{Bmatrix} u_s \\ v_s \\ r_s \\ p_s \end{Bmatrix}; \quad \{\eta\} = \begin{Bmatrix} dx_s \\ dy_s \\ \psi_s \\ \phi_s \end{Bmatrix} \quad (14)$$

In order to overcome some non linearities, like “ $v.r$ ”, “ $u.r$ ”, “ $p.r$ ” and “ $r^2$ ” (Equation 11) it was necessary to consider some of these variables as constant. During the numerical solution process, the values of these variables were being updated step by step.

### 3. Results

The vehicle data are shown in Table 1.

To overcome the nonlinearities, the curves were fitted using straight-line approximations during small increment of time.

The roll axis was obtained using the roll center of the front and rear suspensions and the procedures described by Milliken and Milliken (1995).

The experimental data was acquired using a signal analyzer “Spectra” (model ST7000) with 40 channels, an accelerometer “Entran” (Model – EGCS3 – D – 20 / V10) and five displacement sensors “Celesco” (Model– PT101 – 0040 – 112 – 2120). One displacement sensor was used to acquisition of the steering angle.

It is assumed that the vehicle is travelling, over a flat road, at uniform forward speed,  $U$ , when the driver turns the steering wheel. Figure 3 shows a typical experimental signal of the accelerometer placed at the gravitational center in lateral direction. Figure 4 shows the steering angle obtained through a potentiometer placed in the steering shaft. It is possible to note that the signals are contaminated by others vibration sources like engine and road vibrations.

Table 1 – Vehicle data

$m_s = 14400$ kg	$CK = 82000$ N/m (front axle – left and right)
$m_u = 887$ kg (front axle)	$CK = 2 \cdot 81000$ N/m (rear axle – left and right)
$m_u = 1366$ kg (rear axle)	$CD = 39370$ Ns/m (front axle – left and right)
$I_x = 16279$ kg.m <sup>2</sup>	$CD = 38415$ Ns/m (rear axle – left and right)
$I_y = 132878$ kg.m <sup>2</sup>	$\mu = 0.85$
$I_z = 145766$ kg.m <sup>2</sup>	$T_w = 2.022$ m (front axle)
$I_{x_s} = 376$ kg.m <sup>2</sup>	$T_w = 1.90$ m (rear axle)
$I_{z_s} = 651$ kg.m <sup>2</sup>	$R_t = 0.49$ m
$x_{p_T} = 4.4$ m (front)	$I_t = 46.5$ kg.m <sup>2</sup> (front axle)
$x_{p_T} = -2.3$ m (rear)	$I_t = 2 \cdot 46.5$ kg.m <sup>2</sup> (rear axle)
$y_{p_T} = 1.011$ m (front-right)	$CL_T = 267380$ N/rad (front tires)
$y_{p_T} = -1.011$ m (front-left)	$CL_T = 2 \cdot 267380$ (rear tires)
$y_{p_T} = 0.95$ m (rear-right)	$Ci_T = 990000$ N/unit slip (front tires)
$y_{p_T} = -0.95$ m (rear-left)	$Ci_T = 2 \cdot 890000$ N/unit slip (rear tires)
$h_{CG} = z_{p_{CG}} = 1.4$ m	$\varepsilon_r = 0.015$
$a = 4.4$ m	$b = 2.3$ m

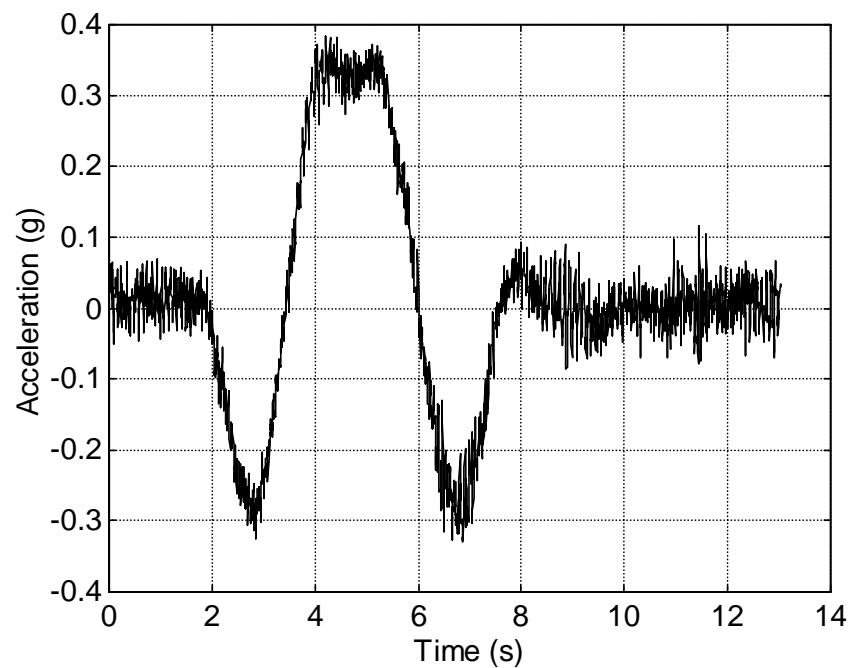


Figure 3. Lateral acceleration

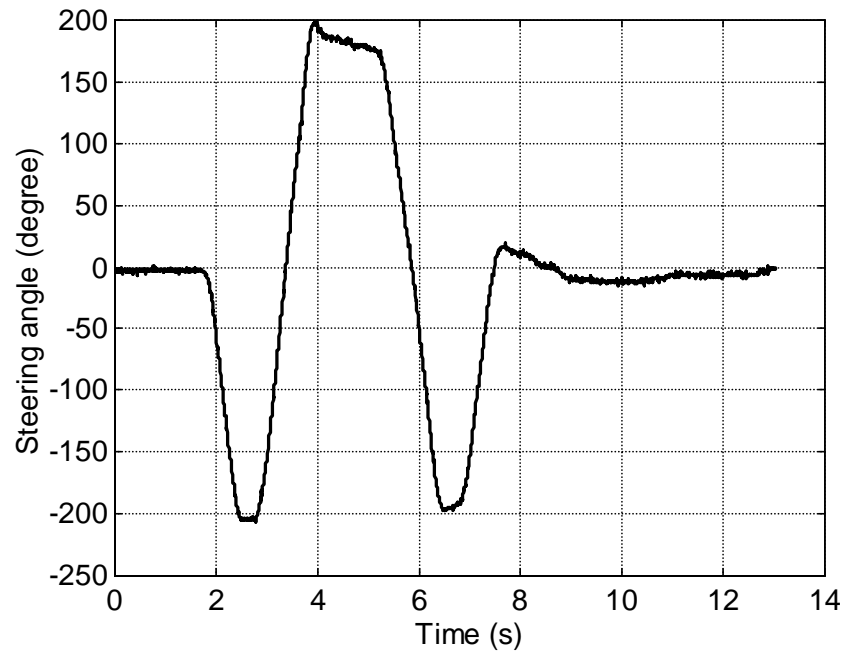


Figure 4. Steering angle

Figure 5 shows the acceleration signal at the frequency domain. Two peaks are evidenced. To eliminate the influence of the vertical movement and the high frequency sources, the signals were filtered using low pass filter (cutoff frequency of 5 Hz). The filtered steering angle signal was utilized to input for the computational simulations.

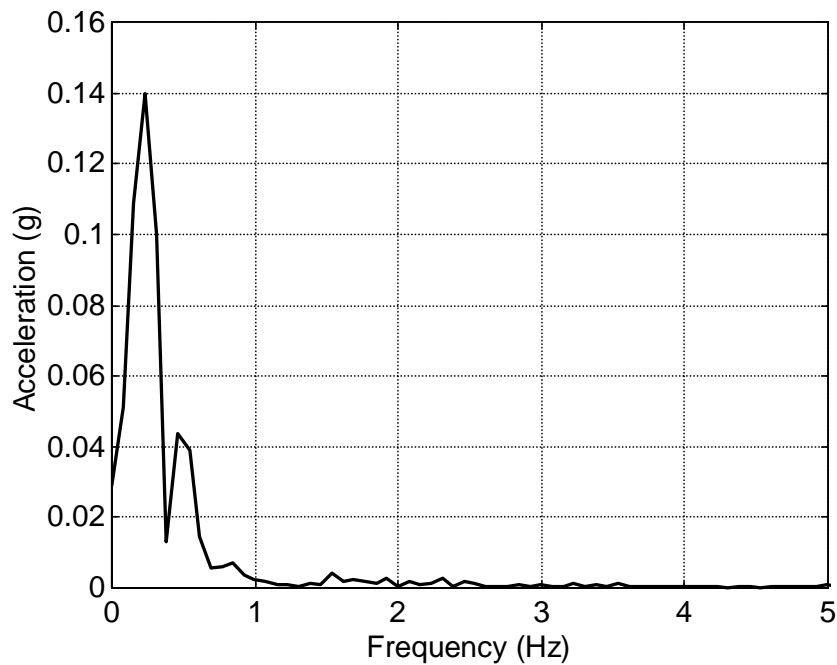


Figure 5. Spectral density of vertical acceleration

The experimental data are obtained using the vehicle forward speed as 20, 40, 50 and 60 km/h. Four displacement sensors are placed in the suspensions and one acceleration sensor is placed in the gravitational center at lateral direction.

Figures 6 and 7 shown the experimental and simulated results. It can be noticed that the experimental and simulated results presents good agreement. At the vehicle speed of 20 km/h it was verified a little resonance with the excitation of

the vertical movement of the front suspension. This fact introduced errors in the experimental roll angle. The lateral acceleration increased with the increment of vehicle speed, assuming values from 0.14 up to 0.6 g. The roll angle presented the same behavior, assuming values from 1.7 up to 3.6 degrees.

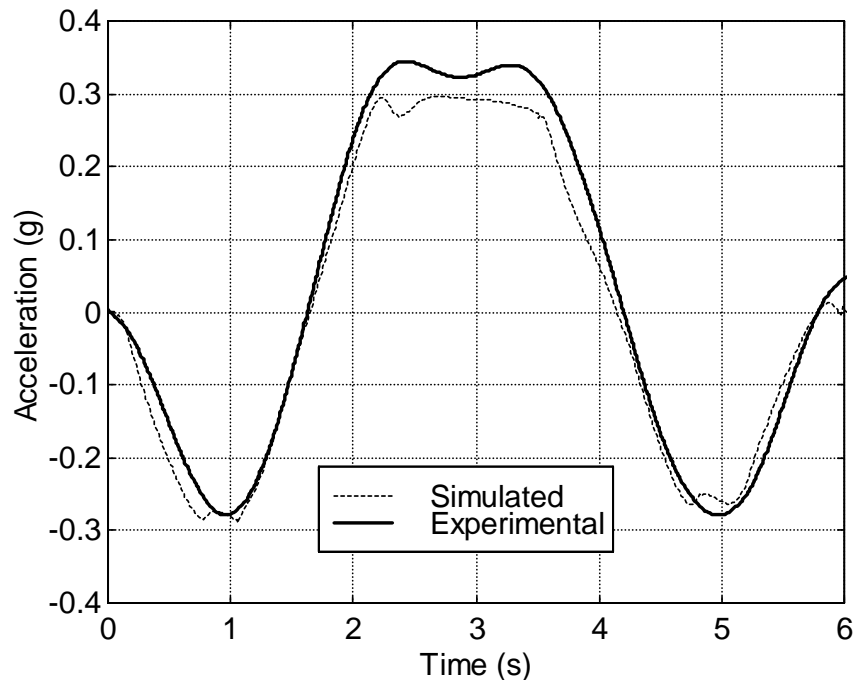


Figure 6. Lateral acceleration (  $v = 40$  km/h )

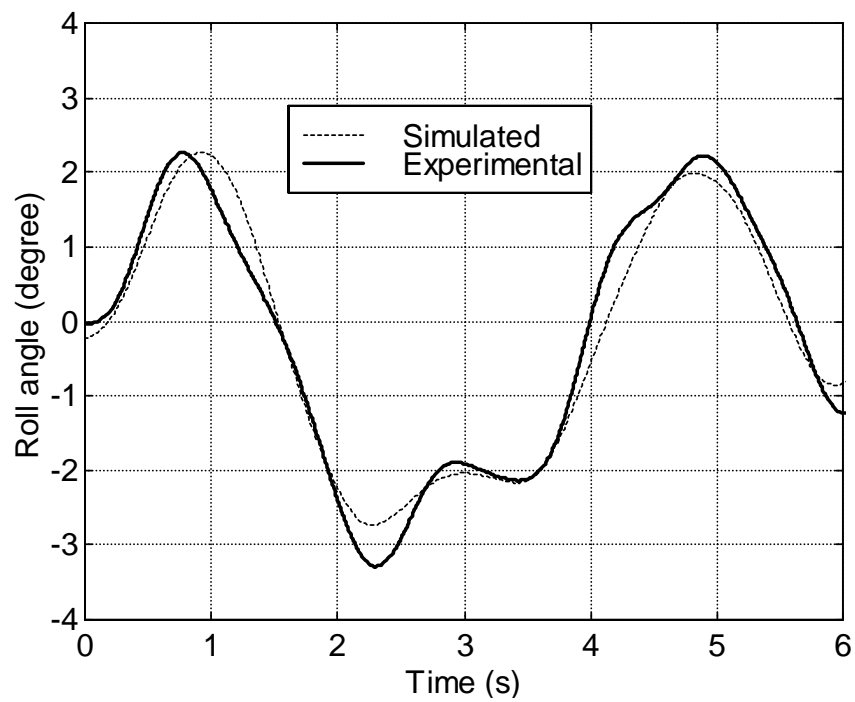


Figure 7. Roll angle (  $v = 40$  km/h )

#### 4. Conclusions

The dynamical performance of a bus, under directional maneuver over a flat road, was analyzed through a physical model with eight degrees of freedom. The mathematical model was validated through comparisons of experimental and simulated data. The results presented good agreement between the data.

At the vehicle speed of 20 km/h it was verified a little resonance with the excitation of the vertical movement of the front suspension. The greater divergences occur in this case.

The filtering of the experimental data showed be a good tool for validation of the numeric models.

#### 5. References

- Nardelo, A., Benicá, L. A. and Vargas, V. M. (2000) 'Suspension performance', *SAE- Suspension Colloquium*, pp. 26-47, Caxias do Sul-Brazil.
- Allen, R. W., Chrstos, J. P., Howe, G., Klyde, D. H., Rosenthal, T. J. (2002) 'Validation of a non-linear vehicle dynamics simulation for limit handling', *Proc. Instn. Mech. Engrs.*, Vol. 216(D), pp. 319-327.
- Allen, R. W., Rosenthal, T. J. and Szostak, H. T. (1987) 'Steady state and transient analysis of ground vehicle handling', *SAE paper No. 870495*.
- Brach, R. M. (1991) 'Vehicle dynamics model for simulation on a microcomputer', *Int. J. of Vehicle Design*, Vol. 12, No. 4, pp. 404-419.
- Diaz, V., Fernandez, M. G., Roman, J. L. S., Ramirez, M., Garcia, A. (2004) 'A new methology for predicting the rollover limit of buses', *International Journal of Vehicle Design*, Vol. 34, No. 4, pp. 340-353.
- Shiller, Z. and Sundar, S. (1998) 'Emergency lane-change maneuvers of autonomous vehicles', *ASME Journal of Dynamic Systems, Measurements and Control*, Vol. 120, No. 1, pp. 37-44.
- Ramanata, P. (1998) 'Optimal Vehicle Path Generator Using Optimization Methods', Master dissertation, Virginia Polytechnic Institute and State University.
- Smith, E. D. and Starkey, J. M. (1995) 'Effects of model complexity on the performance of automated vehicle steering controllers: model, development, validation and comparison', *Vehicle Systems Dynamics*, Vol. 24, pp. 163-181.
- Lee, U. and Han, C. (2001) 'A suspension system with a variable roll center for the improvement of vehicle handling characteristics', *Proc. Instn. Mech. Engrs.*, Vol. 215 (D), pp. 677-696.
- Lee, S. H., Lee, U. K. and Han, C. S. (2001) 'Enhance of vehicle handling characteristics by suspension kinematic control', *Proc. Instn. Mech. Engrs.*, Vol 215(D), pp. 197-216.
- Jung, H., Kwak, B. and Park, Y. (2002) 'Improving the directional stability of a tracton control system without additional sensors', *Proc. Instn. Mech. Engrs.*, Vol. 216 (D), pp. 641-648.
- Kwak, B. and Park, Y. (2001) 'Robust vehicle stability controller based on multiple sliding mode control', *SAE World Congress*, pp. 1-7, Detroit.
- Mangialardi, L. and Mantriota, G. (2001) 'Stability of an articulated vehicle with suspended cargo', *Heavy Vehicle Systems*, A Series of the *Int. J. of Vehicle Design*, Vol. 8, No. 1, pp. 83-102.
- Milliken, W. F. and Milliken, D. L. (1995) 'Race car vehicle dynamics'. Warrendale: Society of Automotive Engineers.
- Ellis, J. R. (1994) 'Vehicle handling dynamics'. London: Mechanical Engineering Publications.

#### 6. Responsibility notice

The authors are the only responsible for the printed material included in this paper.